

## DEVELOPMENT OF A SINGLE CELL $Ca^{2+}$ IMAGING SYSTEM TO STUDY THE ROLE OF PKC SUBSTRATE B-50 IN NEUROTRANSMITTER RELEASE AND NEURITE OUTGROWTH

J. Elands, W.H. Gispen, W.H. and P.N.E. De Graan<sup>1</sup>  
Division of Molecular Neurobiology  
Rudolf Magnus Institute  
Padualaan 8  
3584 CH Utrecht  
The Netherlands

### Introduction

One of the well-characterized substrates of protein kinase C (PKC) in neurons is the protein B-50. B-50 is a nervous tissue-specific substrate of PKC associated with the cytosolic face of the presynaptic membrane (see De Graan et al., 1991). Protein B-50 is identical to the growth-associated protein GAP-43, the calmodulin (CaM)-binding protein neuromodulin, and protein F1, which is implicated in long-term potentiation (for a review see Skene, 1989). B-50 is one of the abundant proteins in the neuronal growth cone (Skene, 1989) and has been implicated in signal transduction and the mechanism of neurite outgrowth during development and differentiation (Skene, 1989). In a series of studies we have shown that the degree of PKC-mediated phosphorylation of B-50 in hippocampal slices and synaptosomes is correlated with transmitter release (Dekker et al., 1991a; Heemskerk et al., 1989,1990). Based on these correlative studies and the fact that phorbol esters which stimulate PKC enhance neurotransmitter release (see Dekker et al., 1991a), we have suggested that PKC-mediated B-50 phosphorylation may be involved in the regulation of neurotransmitter release.

More direct evidence for a role of B-50 in noradrenaline (NA) release was obtained in studies using synaptosomes permeated with the toxin streptolysin-O (SL-O; Dekker et al., 1989;1991b; De Graan et al., 1991). NA release from permeabilized synaptosomes could be induced by elevation of the  $Ca^{2+}$  concentration in the permeation buffer. We have used these permeated synaptosomes to introduce antibodies to B-50, which are known to inhibit B-50 phosphorylation. The affinity purified anti-B-50 IgGs completely inhibited  $Ca^{2+}$ -induced NA release from the permeated synaptosomes (Dekker et al., 1989). Since the antibodies inhibit B-50 phosphorylation, these data indicate that B-50 phosphorylation is important for NA release. However, it is also possible that the antibodies inhibit other properties of the B-50

---

<sup>1</sup>To whom correspondence should be addressed.

molecule besides its PKC-mediated phosphorylation. In fact, we have evidence that PKC inhibitors do not inhibit  $\text{Ca}^{2+}$ -induced release from permeated synaptosomes (De Graan et al., 1991). An interesting possibility is the CaM binding property of B-50. It has been shown by Storm and co-workers that purified B-50 has a higher affinity for CaM in the absence of  $\text{Ca}^{2+}$  than in the presence (for a review see Liu and Storm, 1990) and that prephosphorylation of purified B-50 by PKC inhibits CaM binding. Based on these *in vitro* studies it has been suggested that *in vivo* B-50 may act as a local CaM store. CaM may be dissociated from B-50 after a depolarization-induced rise in intracellular  $\text{Ca}^{2+}$  and subsequently activate cellular processes involved in transmitter release, for instance CaM-dependent kinases and phosphorylation of synapsin I (Nichols et al., 1990). Once CaM and B-50 have been dissociated, B-50 may be phosphorylated by PKC, thus preventing reassociation of CaM and prolonging CaM action. Indeed, we could recently show (De Graan et al., 1990,1991) that using the chemical crosslinker disuccinimidyl suberate a complex can be detected between CaM and endogenous B-50 in native SPM and growth cone membranes. This complex formation is regulated by the free  $\text{Ca}^{2+}$  concentrations which occur under physiological conditions in neurons.

Interestingly, the concentrations of  $\text{Ca}^{2+}$  required to induce NA release and dissociation of the B-50/CaM complex (up to  $10^{-5}$  M) in permeated synaptosomes are much higher than those measured in intact synaptosomes using the fluorescent  $\text{Ca}^{2+}$  indicator Fura-2. The high  $\text{Ca}^{2+}$  concentration necessary to induce release contrasts with the overall  $\text{Ca}^{2+}$  levels measured after  $\text{K}^+$  depolarization of intact synaptosomes, which do not exceed the  $0.5 \times 10^{-6}$  M level (Verhage et al., 1988). There are two explanations for this apparent contradiction: (i) local high levels of  $\text{Ca}^{2+}$  are required to induce transmitter release, and (ii) high concentrations of  $\text{Ca}^{2+}$  are necessary in the permeated system to overcome SL-O-induced damage to the release machinery, or to overcome dilution of cytosolic components of the release system. Extremely high local  $\text{Ca}^{2+}$  concentrations would occur just below the plasma membrane immediately following depolarization when  $\text{Ca}^{2+}$  enters through voltage sensitive  $\text{Ca}^{2+}$  channels (VSCC). If B-50 is involved in the release mechanism the prediction would be that for instance changes in the degree of phosphorylation would parallel a  $\text{Ca}^{2+}$  influx rather than an overall increase in the  $\text{Ca}^{2+}$  concentration. A series of experiments using different depolarization techniques in intact synaptosomes indeed provide evidence for a close correlation between  $\text{Ca}^{2+}$  influx and B-50 phosphorylation (Heemskerk et al., 1991; De Graan et al., 1991).

The notion that B-50 function maybe directly regulated by local  $\text{Ca}^{2+}$  concentrations

in synaptosomes and possibly also in growth cones has prompted us to develop a single cell  $\text{Ca}^{2+}$  imaging system to monitor local differences in  $\text{Ca}^{2+}$  concentrations in individual neurons and measure effects of modulation of the B-50/PKC/CaM system on  $\text{Ca}^{2+}$  parameters.

### Single cell $\text{Ca}^{2+}$ imaging system

Several techniques are available to study  $\text{Ca}^{2+}$  concentrations or  $\text{Ca}^{2+}$  flows;  $\text{Ca}^{2+}$  sensitive electrodes,  $^{45}\text{Ca}^{2+}$  flow measurements, intracellular recording using patch clamp and  $\text{Ca}^{2+}$  sensitive fluorochromes. While patch clamp recording,  $\text{Ca}^{2+}$  electrodes and  $^{45}\text{Ca}^{2+}$  flow measurements are promising techniques, the use of the second generation of fluorochromes in combination with video microscopy is the only technique enabling the measurement of  $\text{Ca}^{2+}$  concentrations in living cells with complex morphology under nearly physiological conditions.

The most successful compound in the first generation of fluorochromes was quin2, which has been widely used to measure  $\text{Ca}^{2+}$  level changes in dissociated and/or cultured cells, either using a spectrofluorimeter, fluorescence microscope equipped with a photomultiplier or a video camera. However, quin2 had several disadvantages over the second generation of  $\text{Ca}^{2+}$  fluorochromes (Grynkiewicz et al., 1985), of which fura-2 is the most commonly used. The new probes have a lower affinity for  $\text{Ca}^{2+}$ , thus enabling measurements at higher  $\text{Ca}^{2+}$  concentrations and also limiting buffering capacity, a higher total fluorescence yield, enabling reduction of the UV excitation light intensity and faster kinetics. Moreover, the selectivity for  $\text{Ca}^{2+}$  over other divalent metal cations ( $\text{Mg}^{2+}$ ) has been substantially improved, while cations like  $\text{Mn}^{2+}$  can still be used to quench fura-2 completely (Grynkiewicz et al., 1985). Since cell membranes are impermeable for hydrophilic substances as fura-2 (and quin2), they have to be injected into the cell, or be presented in a more lipophilic form. The acetoxymethylester derivative, fura-2/AM, is able to pass the cell membrane to enter the cytoplasm where esterases convert it into free fura-2. This hydrolysis is not always complete (Schmidt et al., 1988), therefore  $\text{Ca}^{2+}$  insensitive but highly fluorescent metabolites of fura-2/AM may be present. The most important feature of fura-2 (and indo-1) over quin2 however is a shift in excitation (emission for indo-1) spectrum upon  $\text{Ca}^{2+}$  binding. Fura-2 can be more readily excited at 340 nm when it has bound  $\text{Ca}^{2+}$  and at 380 nm when it exists in the  $\text{Ca}^{2+}$  free state. The ratio of the fluorescence at these two wavelengths can be used to determine the exact  $\text{Ca}^{2+}$  concentration (Grynkiewicz et al., 1985; Tsien and Poenie, 1986). According to the method proposed by Tsien et al. (Grynkiewicz et al., 1985) the  $\text{Ca}^{2+}$  concentration follows from the following equation:

$$[Ca^{2+}] = K_d * \beta \left( \frac{R_t - R_{min}}{R_{max} - R_t} \right)$$

where the  $K_d$  represents the dissociation constant of fura-2 for  $Ca^{2+}$  (225 nm at 37°C),  $\beta$  the ratio of the limiting minimal and maximal fluorescence levels at 380 nm ( $F_o/F_s$ ),  $R_{min}$  and  $R_{max}$  the 340/380 nm fluorescence ratios at respectively minimal and maximal intracellular  $Ca^{2+}$  concentration and  $R_t$  the 340/380 nm fluorescence ratio at a given pixel and time in a (ratio) image.  $R_{max}$  can be measured after loading the cell with  $Ca^{2+}$  for instance by making the cell membrane permeable for  $Ca^{2+}$  by ionomycin. Then, using EGTA  $R_{min}$  can be determined.

When this approach is combined with computer assisted video microscopy the actual  $Ca^{2+}$  concentration can be visualized in a two-dimensional image (for review see Tsien 1988,1989). An alternative approach, also to be used as a control, is to prepare titrated EGTA/ $Ca^{2+}$  buffers and to measure fluorescence in vitro in flat glass capillaries or microscopic slides. The potential of the use of titrated buffers in ionomycin treated cells has also been put forward (Williams et al., 1985), but limitation of bulk volume  $Ca^{2+}$  transport through the ionomycin formed pores limits the use of this approach.

From the characteristics and dynamics of the above described B-50/PKC/CaM model several aspects of the ratio-imaging technique can be inferred. -  $Ca^{2+}$  concentrations in nerve cells are rapidly changing, the system should thus be able to capture data at a relatively high speed. - Since B-50 is a presynaptic protein, localized in axons, growth cones and in presynaptic terminals, measurements must be done in structures that are very small and will thus have a low fluorescence yield. A very sensitive video camera is necessary, in conjunction with a microscope generating virtually no background light. - Living cells are used that must be maintained for periods up to several hours under physiological circumstances. This can only be achieved in appropriate (specially designed) tissue culture chambers thermostatically controlled by a heating element and/or a perfusion system.

#### *Technical aspects (Fig. 1)*

##### **Microscope**

Essentially two types of microscopes exist for fura-2 measurements. The normal fluorescence and the epifluorescence microscope. The first type uses objectives with extra long working distance that are immersed into the cell culture medium. The excitation beam

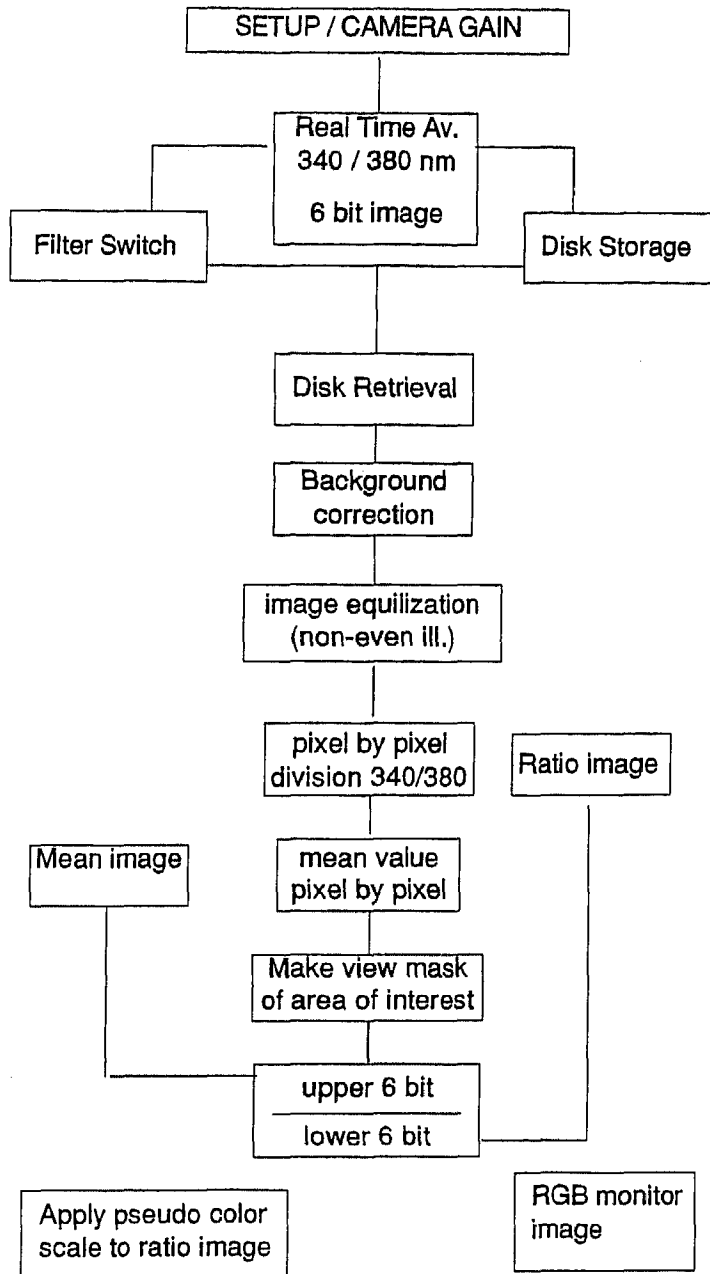


Fig. 1. A flow chart of the  $\text{Ca}^{2+}$  imaging equipment.

enters the object via the bottom or via UV fibre optics. For fura-2 measurements no fluor lenses are necessary since the emission peak of fura-2 is in the visible light wavelength range. However, this approach renders it impossible to introduce additional tools as patch-clamp electrodes or micro-pipette devices. Therefore an epifluorescence microscope (we use a Nikon Diaphot TMD) is a better alternative. Since the objectives in this microscope approach the specimen from the bottom side, the UV excitation light must be transported via the objectives in order to avoid restrictions to use additional tools. The light from the UV source is reflected to the objectives by a 400 nm dichroic mirror. The emitted light passes the objectives, the dichroic mirror and a 510 nm barrier filter to eliminate light from other sources than fura-2 and can then be visualized in the binocular or the video camera. A 100%-100% changer between the camera and the binocular should be present to have all the light available at the camera. All the optical components of the epifluorescence microscope must be of UV quartz glass since normal optics have a cut off wavelength well above 340 nm.

#### **UV source**

Both xenon and mercury UV sources can be used. However, the spectral distribution of both devices is greatly different. The mercury lamp we use has a very pronounced 360 nm line in its spectrum that one has to be aware of. Generally the produced light spectra are very sensitive to small voltage changes so that a very stable power supply is essential.

The wide ranging UV spectra of the UV source is transformed into narrow band 340 and 380 nm light by two interference filters. Generally these filters have a 5 to 20 nm bandwidth. The all-over efficiency of the filter determines the amount of light that is transmitted. It is therefore of importance that a set of calibrated filters (preferably in conjunction with the UV source) is obtained so that both wavelengths give approximately the same fluorescence yield at medium  $\text{Ca}^{2+}$  concentrations. Quartz neutral density filters can be used to correct for imbalances. Generally these filters are mounted in a switch device that is computer driven to be in phase with the image acquisition. In order to reduce fura-2 bleaching the UV light has to be shut off immediately after a determination. This can be done by incorporating an electronic shutter in the optical path. However, fura-2 bleaching may even then be a problem (Becker and Fay, 1987).

#### **Video camera**

To visualize fura-2 emission CCD intensified cameras are a good choice. In a

relatively affordable way sensitivities of  $10^{-7}$  lux can be obtained which are necessary for measurements in axons and growth cones. The class of cooled intensified CCD cameras is not only very sensitive but also have an extremely low dark-current (background light or noise) and a large dynamic range ( $> 1000$ ). These cooled cameras are however rather slow (slow-scan camera), i.e. the generation of a single image needs a scan time in the order of the 100 msec range. The non-cooled intensified CCD cameras (we use a MX-II, HCS, NL), working at ambient temperature, have scan times of 10 to 30 msec, enabling to work at video rate (25 images per second in Europe, 30 in the USA). However, they have a limited dynamic range 60-200 and a higher dark-current. As will be discussed later the real dynamic range is also dependent on the video frame capture board (frame grabber) or the real time average device.

Intensified CCD cameras are easily damaged by exposure to extreme amounts of light. Therefore it is highly recommended to mount an electronic shutter between the camera and the microscope housing to avoid accidental overexposure. For a general review on video microscopy see Inoué (1987).

#### **Video frame capture board or frame grabber**

When cameras are used that function according to industrial video standards they generate an analogous output signal. To use such a signal for measurements and calculations it must first be converted into a digital form. A frame grabber converts analogous signals continuously into digital signals. The resulting digital images can be manipulated by a computer. However, at low light levels, a single digitized image is usually of a rather poor quality due to heavy noise influence. To reduce the noise averaging of several images in the time can be done. Frame grabber devices either provide a slow averaging mode (often in conventional computer memory) or a fast, real-time averaging mode. The latter mode has the advantage of speed and temporal resolution since no images are left unused for the averaging process.

The dynamic range of frame grabbers is defined as the number of bits available to code the incoming grey values. As the early systems sometimes used only 3 or 4 bits (dynamic range from 8 to  $16, 2^n$  where  $n$  is the number of bits) most modern systems use 6 to 8 bits, with exceptions using 16 to 24 bits. We use a frame grabber (FG-100 board, Imaging Technology Inc., USA) that has an 8 bit dynamic range for normal purposes and a 6 bit range for real time averaging (total memory is 12 bits, for real time averaging 6 bits are

used for the average buffer and 6 for the incoming signal). Although a 6 bit dynamic range seems limiting one must consider the dynamic range of the camera ( $\pm 100$ ) in relation to the range of the frame grabber. One point worth mentioning in this respect is that the system needs careful tuning of the camera gain in order to adjust the dynamic range of the camera to that of the frame grabber.

### **Image storage, computers**

The storage of images is dependent on the video frame grabber specifications (image size and number of bits dynamic range) and experimental conditions (acquisition speed or time resolution and (sub)image size). Standard images at this moment are  $256^2$  pixel images and 8 bit dynamic range, although the trend is towards  $512^2$  pixel images.  $256^2$  pixel images by 8 bit (which we use) give rise to 64 Kilobytes of information, while  $512^2$  pixel images result in 256 Kb data files. This relatively large image file size imposes restrictions on the speed of data storage on computers. When standard "state of the art" IBM-PC computer hardware is used only 1 to 4 image files (64 Kb) per second can be stored. This is sufficient to measure low speed  $\text{Ca}^{2+}$  changes. We use a 486 25 mHz PC with a fast 660 Mb harddisk. Generally data images are stored before processing. This saves time during the acquisition sequence when the original data images are to be stored. In case ratio images are directly determined, processing before storage can be advantageous in terms of speed but obviously access to the original "raw" data is lost. For high speed purposes recording onto high quality industrial video recorders (e.g. the Sony UMATIC with frame code generator we use, or industrial super VHS systems) and digitalization and analysis afterwards can provide a good alternative. Using these standard techniques (at video frame rate) maximal 25 images (30 in USA) per second can be recorded on tape. The disadvantages are obvious, no possibility of real time average mode (due to maximal speed storage) and loss of image quality.

### **Image processing software**

The coordination of filter switch devices (we use the Lambda 10 switcher from Sutter Instrument Co., USA), electronic shutters and the acquisition and processing of image data is taken care of by a computer program. Such a program can either be an adapted version of existing image manipulation software (we used TIM digital image processing software, DIFA Measuring Systems, Breda, NL) or a highly specialized custom written package. The most essential functions needed are: image correction for background illumination and uneven



illumination; ratio determination using the 340 and 380 nm images; pseudocolour display of images with a calibrated color scale; area, point and line measurements of  $\text{Ca}^{2+}$  concentrations. An enormous amount of nice and fancy tricks can be offered to the experimenter, i.e. 3 dimensional plots of images, combinations of plots and pseudocolour images etc. Although these options can be useful they are not essential for  $\text{Ca}^{2+}$  measurements using the ratio approach.

### *Biological aspects*

#### **Methodology**

$\text{Ca}^{2+}$  measurement by means of fluorescent probes is rather sensitive to temperature changes, while pH changes, when restricted to the range of pH 6.75 to 7.05 appear to have no significant influence on the fluorescence. However, it is advisable to strictly control for both pH and temperature. Buffer pH can be nicely set using a oxygenated Hepes Krebs-Ringer buffer, which, in combination with a good perfusion system, can also perfectly control the temperature. In addition the culture dish can be placed in a heating element with a thermostatic control. Such a controlled heating device can also be used to control temperature in non-perfused steady state conditions. The evaporation of medium can be overcome by a special coating of oil on top of the medium, that is permeable to gasses but not to water. The control of the temperature by the thermostatic device should not take place by switching on and off the current to the heating element since this can result in electronic noise rendering electrophysiological measurements impossible. Regulating the heating element voltage is a more appropriate method. Ideally the microscope objective should be at about the same temperature as the culture dish.

Fura-2/AM loading properties of cells are variable, and need to be assessed carefully since the way of loading may affect the  $\text{Ca}^{2+}$  measurements dramatically (Almers and Neher, 1985). Fura-2/AM also penetrates cell compartments, especially when the de-esterification is slow and incomplete. When micro-injection techniques or patch-pipettes are used, fura-2 can be introduced directly into the cell.

Using our  $\text{Ca}^{2+}$ -imaging system, changes in intracellular  $\text{Ca}^{2+}$  concentrations have been monitored in different cell lines, e.g. in the rat pheochromocytoma cell line PC-12. Resting PC-12 cells, treated for 24 h with Nerve Growth Factor, have a basal intracellular  $\text{Ca}^{2+}$  concentration of approximately 100-200 nM (Fig 2a, c). Upon potassium ( $\text{K}^+$ , 20 mM)-induced depolarization intracellular  $\text{Ca}^{2+}$  levels quickly rise to 500-700 nM. The  $\text{Ca}^{2+}$

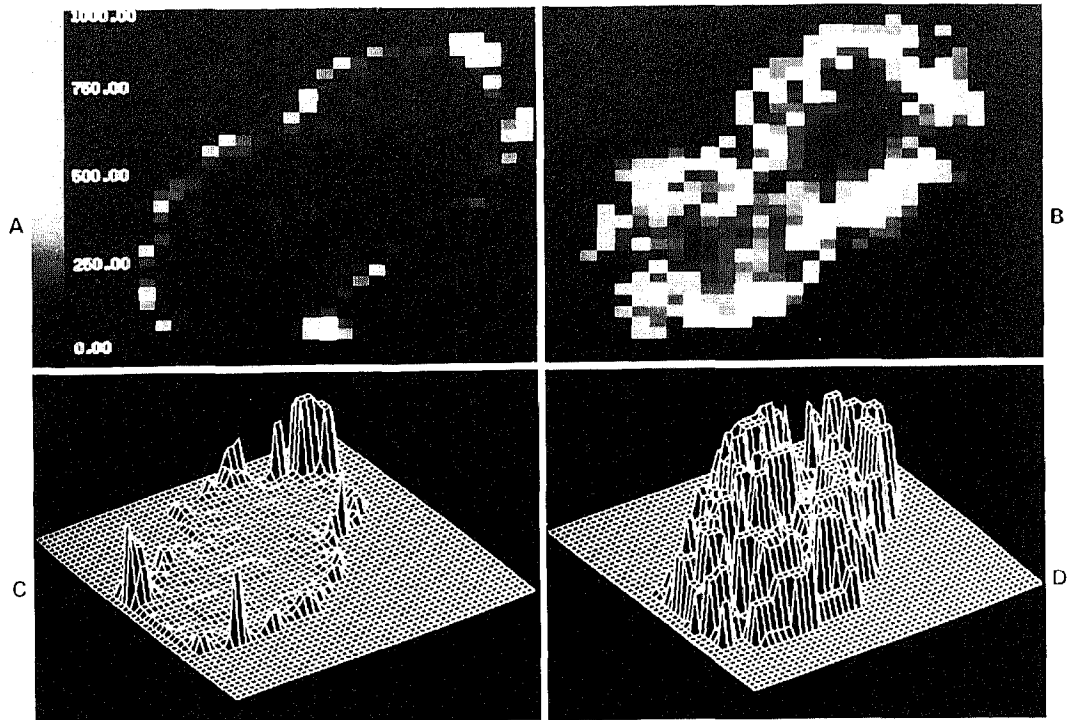


Fig. 2. PC-12 cells before (a, c) and after (b, d) a 20 mM  $K^+$  stimulus. Upper panels, black and white representation of  $Ca^{2+}$  concentrations, black represents 0 nM while white represents concentrations above 1000 nM. Lower panels are 3D plots of the cells shown in the upper panels. The  $Ca^{2+}$  concentration is 100-200 nM under resting conditions (a,c). After the  $K^+$  stimulus the  $Ca^{2+}$  concentration increases up to 700-1000 nM.

concentration begins to increase at the cell membrane region and thus an intracellular  $\text{Ca}^{2+}$  concentration gradient develops, eventually leading to a more uniform concentration. After several tens of seconds  $\text{Ca}^{2+}$  concentrations even ranged from 700 to 1000 nM (Fig. 2b, d). The  $\text{Ca}^{2+}$  concentration remained elevated for several minutes after  $\text{K}^+$  addition and then slowly returned to basal levels. Not all cells respond in the same way, some cells were nearly not excitable, while some others reacted only faintly upon  $\text{K}^+$  addition.

In conclusion the fura-2 ratio approach to measure  $\text{Ca}^{2+}$  concentrations in living cells is a powerful technique that can be combined with electrophysiological (patch-clamp) measurements. The addition of video microscopy enables to monitor changes in  $\text{Ca}^{2+}$  gradients with high spatial and temporal resolution. This technique greatly enhanced the understanding of the role of  $\text{Ca}^{2+}$  changes in strictly localized cell regions (Cheek et al., 1989; Connor et al., 1987; Connor, 1986; Williams et al., 1985). Although the method demands considerable investments a great variety of problems can be investigated, that are not only related to  $\text{Ca}^{2+}$  concentrations. In the same family of fluorochromes several other dyes, sensitive for pH, membrane potential,  $\text{Na}^+$ ,  $\text{Cl}^-$  etc. are available (see Tsien, 1989 for review) and a new generation of dyes, possibly also for other second messengers, can be expected in the near future.

#### Acknowledgments

We thank DIFA Measuring Systems (Breda, NL) for their support and the development of the  $\text{Ca}^{2+}$  imaging software. J. Elands was supported by Tropon Werke GmbH (Cologne, Germany).

#### REFERENCES

- Almers W, Neher E (1985) The calcium signal from fura-2 loaded mast cells depends strongly on the method of dye-loading. *FEBS Lett* 192: 13-18.
- Becker PL, Fay FS (1987) Photobleaching of fura-2 and its effect on determination of calcium concentrations. *Am J Physiol* 253: C613-C618.
- Cheek TR, O'Sullivan AJ, Moreton RB, Berridge MJ, Burgoyne RD (1989) Spatial localization of the stimulus-induced rise in cytosolic  $\text{Ca}^{2+}$  in bovine adrenal chromaffin cells. Distinct nicotinic and muscarinic patterns. *FEBS Lett* 247: 429-434.
- Connor JA (1986) Digital imaging of free calcium changes and of spatial gradients in growing processes in single, mammalian central nervous system cells. *Proc Natl Acad Sci USA* 83: 6179-6183.
- Connor JA, Cornwall MC, Williams GH (1987) Spatially resolved cytosolic calcium response to angiotensin II and potassium in rat glomerulosa cells measured by digital imaging techniques. *J Biol Chem* 262: 2919-2927.

- De Graan PNE, Oestreicher AB, De Wit M, Kroef M, Schrama LH, Gispen WH (1990) Evidence for the binding of calmodulin to endogenous B-50 (GAP-43) in native synaptosomal plasma membranes. *J Neurochem* 55: in press.
- De Graan PNE, Schrama LH, Oestreicher AB, Schotman P, Gispen WH (1991) Protein kinase C substrate B-50 (GAP-43) and neurotransmitter release. *Progr Brain Res*, in press.
- Dekker LV, De Graan PNE, Oestreicher AB, Versteeg DHG, Gispen WH (1989) Inhibition of noradrenaline release by antibodies to B-50 (GAP-43). *Nature* 342: 74-76.
- Dekker LV, De Graan PNE, Gispen WH (1991a) Transmitter release: target of regulation by protein kinase C? *Progr Brain Res*, in press.
- Dekker LV, De Graan PNE, Pijnappel P, Oestreicher AB, Gispen WH (1991b) Nor-adrenaline release from streptolysin-O-permeated rat cortical synaptosomes. *J Neurochem*, in press.
- Grynkiewicz G, Poenie M, Tsien RY (1985) A new generation of  $Ca^{2+}$  indicators with greatly improved fluorescence properties. *J Biol Chem* 260: 3440-3450.
- Heemskerk FMJ, Schrama LH, Gianotti C, Spierenburg H, Versteeg DHG, De Graan PNE, Gispen WH (1989a) 4-Aminopyridine stimulates B-50/GAP-43 phosphorylation and [ $^3H$ ]-noradrenaline release in rat hippocampal slices. *J Neurochem* 54: 863-869.
- Heemskerk FMJ, Schrama LH, De Graan PNE, Gispen WH (1990) 4-Aminopyridine stimulates B-50 (GAP-43) phosphorylation in rat synaptosomes. *J Mol Neurosci* 2: 11-17.
- Heemskerk FMJ, Schrama LH, Ghijsen WEHM, De Graan PNE, Lopes da Silva FH, Gispen WH (1991) Presynaptic mechanism of action of 4-aminopyridine: changes in  $[Ca^{2+}]_i$  and its relationship to B-50 (GAP-43) phosphorylation. *J Neurochem*, in press.
- Inoue S (1987) *Video Microscopy*. Plenum Press, NY.
- Liu Y, Storm DR (1990) Regulation of free calmodulin levels by neuromodulin: neuron growth and regeneration. *Trends Pharmacol Sci* 11: 107-111.
- Nichols RA, Sihra TS, Czernik AJ, Nairn A, Greengard P. (1990) Calcium/calmodulin-dependent protein kinase II increases glutamate and noradrenaline release from synaptosomes. *Nature* 343: 647-651.
- Schmidt D, Papadopoulos MT, Crooke ST, Stassen FL (1988) Potential role of protein kinase C in the regulation of vasopressin ( $V_1$ ) receptors of vascular smooth muscle cells (A10) *Faseb J* 2: A624.
- Skene JHP (1989) Axonal growth-associated proteins. *Ann Rev Neurosci* 12: 127-156.
- Tsien RY (1988) Fluorescence measurement and photochemical manipulation of cytosolic free calcium. *TINS* 11: 419-424.
- Tsien RY (1989) Fluorescent indicators of ion concentrations. *Meth Cell Biol* 30: 127-156.
- Tsien RY, Poenie M (1986) Fluorescence ratio imaging: a new window into intra-cellular ionic signalling. *Trends Biochem Sci* 11: 450-455.
- Verhage M, Besselsen E, Lopes da Silva FH, Ghijsen WEJM (1988) Evaluation of the  $Ca^{2+}$  concentration in purified nerve terminals: relationship between  $Ca^{2+}$  homeostasis and synaptosomal preparation. *J Neurochem* 51: 1667-1674.
- Williams DA, Fogarty KE, Tsien RY, Fay FS (1985) Calcium gradients in single smooth muscle cells revealed by the digital imaging microscope using fura-2. *Nature* 318: 558-561.